

# Neural Network Dynamics



**Arjit Kant Gupta**

Department of Physical Sciences

Indian Institute of Science Education and Research, Mohali

A dissertation submitted for the partial fulfillment of  
BS-MS (dual degree in Science)



I would like to dedicate this thesis to my parents who always encouraged and supported me to pursue my interest.



## **Declaration**

The work presented in this dissertation has been carried out by me under the guidance of Dr. Abhishek Chaudhuri, at the Indian Institute of Science Education and Research, Mohali. This work has not been submitted in part or in full for a degree, a diploma, or a fellowship to any other university or institute. Wherever contributions of others are involved, every effort has been made to indicate that clearly. Due acknowledgment of collaborative research and discussions has been made. This thesis is a bonafide record of original work done by me and all sources listed within have been detailed in the bibliography.

Arjit Kant Gupta  
(candidate)

In my capacity as the supervisor of the candidate's project work, I certify that the aforesaid statements by the candidate are true to the best of my knowledge.

Dr. Abhishek Chaudhuri  
(supervisor)

Dated: November 25, 2016



## **Certificate of Examination**

This is to certify that the dissertation titled **Neural Network Dynamics**, submitted by **Mr. Arjit Kant Gupta** (Registration number : MS11073) for the partial fulfillment of the BS-MS dual degree program of the Indian Institute of Science Education and Research, Mohali, has been examined by the thesis committee duly appointed by the institute. The committee finds the work done by the candidate satisfactory and recommends that the report be accepted.

Dr. Somdatta Sinha

Dr. Sudeshna Sinha

Dr. Abhishek Chaudhuri  
(supervisor)

Dated: November 16, 2016





## **Acknowledgements**

I would like to express my sincere gratitude to my project supervisor Dr. Abhishek Chaudhuri for his continuous guidance, support and encouragement for independent thinking. He gave me a chance to work on a project of my own choice and his passion for science always kept me motivated for pushing the limits. I acknowledge the contribution of Dr. Sudeshna Sinha and Dr. Somdatta Sinha for guiding me through the challenges I faced during analysis. I thank Dr. Kavita Babu for giving me chance to work in a neuroscience lab from where I got numerous ideas and also she provided me with the workspace in her lab for my project.

I am thankful to Dr. Yogesh Dahiya and Saurabh Thapliyal for extremely fruitful discussions on neuroscience. Their frank remarks and severe criticism helped me raise my standard to a new level. A special thanks to Kanishk Jain and Mohanlal for discussions related to simulation algorithms.

I thank my friend Amritha Sreekumar for constant love and support. She always believed in my capabilities and kept pushing me to do the best in everything. She never missed a chance to help me in every way she could.

I am grateful to my sisters Ritika Gupta and Vartika Gupta for their emotional support during hard times in my college life. I want to extend a warm thanks to Shivali Sokhi and Bharti Yadav for many enlightening philosophical discussions during campus walks that brought about significant changes in my personality.

At last, I would like to thank Indian Institute of Science Education and Research, Mohali for providing me such an open environment for doing science as well as infrastructural support and INSPIRE for providing me with financial support.



## List of Figures

1.1	(a) Depiction of reticular brain structure, (b) Sketch of real neural network by Ramón y Cajal	1
1.2	(a) Structure of single neuron, (b) Structure of synapse	2
1.3	Structure of a patch of cell membrane	3
1.4	Equivalent RC circuit of cell membrane	4
1.5	Integrate-and-fire model of single neuron and its equivalent circuit diagram	5
1.6	Response of membrane patch to input square pulse at two different membrane time constants( $\tau_m$ ): 20ms and 50ms	6
1.7	Response of single integrate-and-fire neuron to input current pulses of four different amplitudes: 10mA, 20mA, 30mA and 40mA	7
1.8	Frequency – Current (f-I) curve for integrate-and –fire neuron at two refractory periods( $\tau_r$ ): 0ms and 1 ms	9
2.1	Directed network with 8 nodes and 17 edges & corresponding adjacency matrix	11
2.2	Activity of Neuronal population in response to input signal	12
3.1	Average population activity as a function of strength of EPSP (J) at different relative inhibition strengths (g)	17
3.2	Average population activity as a function of strength of EPSP (J) at different average in-degree per neuron (C)	18
3.3	Average population activity as a function of strength of EPSP (J) at different network sizes (N)	19
3.4	Average population activity as a function of strength of EPSP (J) at different membrane time constants ( $\tau_m$ )	20
3.5	Average population activity as a function of strength of EPSP (J) at different refractory periods ( $\tau_r$ )	21
3.6	Average population activity as a function of strength of EPSP (J) at different synaptic time constants ( $\tau_s$ )	22
3.7	Plot of alpha function against time	22
3.8	Histogram of coefficient of variation of ISI distribution at various strengths of EPSP (J) for 10000 neurons	24
3.9	Population activity of the network for Gaussian input pulse in two different network states at (a) J = 0.2mV (b) J = 0.8mV	25
3.10	Population activity of the network for square input pulse in two different network states at (a) J = 0.2mV (b) J = 0.8mV	26
3.11	Population activity of the network for ramp input pulse in two different network states at (a) J = 0.2mV (b) J = 0.8mV	26
3.12	Population activity of the network for sinusoidal input pulse in two different network states at (a) J = 0.2mV (b) J = 0.8mV	27



## Notation

$N$	Number of neurons in the network
$C$	Average in-degree per neuron
$J$	Strength of excitation (EPSP amplitude)
$g$	Relative strength of inhibition to excitation
$\tau_m$	Membrane time constant
$\tau_s$	Synaptic time constant
$\tau_r$	Absolute refractory period of neuron
$\theta$	Firing threshold of the neuron
$V_{\text{reset}}$	Reset potential of the neuron
$C_m$	Membrane capacitance
$R_m$	Membrane resistance
$\mu_0$	Constant offset voltage provided to every neuron
$T$	Total simulation time
EPSP	Excitatory Post Synaptic Potential
IPSP	Inhibitory Post Synaptic Potential
$A$	Population Activity
ISI	Interspike Interval
CV	Coefficient of Variation



# Contents

<b>List of Figures</b>	<b>i</b>
<b>Notation</b>	<b>iii</b>
<b>Abstract</b>	<b>vii</b>
<b>Contents</b>	<b>v</b>
<b>1 Introduction</b>	<b>1</b>
1.1 History of Neural Networks	1
1.2 Biological Neuron	2
1.3 Modelling Neurons as RC circuits	3
1.4 Leaky Integrate-and-Fire Model	4
1.5 Response of Integrate-and-Fire Neuron to Square Pulse	6
1.5.1 Membrane response at various membrane time constants	6
1.5.2 Membrane response at various current amplitudes	7
1.6 Frequency – Current Curve of Integrate-and-Fire Neuron	8
<b>2 Network of Neurons</b>	<b>11</b>
2.1 Networks and Their Representation	11
2.2 The Adjacency Matrix	11
2.3 Population Activity	12
2.4 Homogeneous Population of Integrate-and-Fire Neurons	13
<b>3 Simulations and Results</b>	<b>15</b>
3.1 Network Description and Parameters	15
3.2 Response of Network as a Function of Network Parameters	16
3.2.1 Average population activity vs excitation strength at various $g$ values	17
3.2.2 Average population activity vs excitation strength at various $C$ values	18
3.2.3 Average population activity vs excitation strength at various $N$ values	19
3.2.4 Average population activity vs excitation strength at various $\tau_m$ values	20
3.2.5 Average population activity vs excitation strength at various $\tau_r$ values	21
3.2.6 Average population activity vs excitation strength at various $\tau_s$ values	22
3.3 Splitting of Neural Populations	23
3.4 Network Response to Input Pulses	25
3.4.1 Gaussian Pulse	25
3.4.2 Square Pulse	26
3.4.3 Ramp Pulse	26
3.4.4 Sinusoidal Pulse	27
3.5 Conclusions	27
<b>References</b>	<b>29</b>





## **Abstract**

Over past few years, experimental findings have shown that there exists self-sustained background activity in the cortex of the brain even if the brain is not involved in any kind of task. The role of this activity is not understood till date and has become one of the interesting questions in the field of computational neuroscience. Such activity has been predicted to be a result of competition between excitatory and inhibitory synaptic inputs. In this thesis, we have studied the properties of a homogeneous network of excitatory and inhibitory leaky integrate-and-fire neurons. It was shown in a computational study that such activity can only arise in inhibition dominated regime. We have studied the mean population activity as a function of network parameters such as network size, sparsity, the strength of excitation, the relative strength of inhibition to excitation, refractory period, membrane time constant and synaptic time constant. We confirmed the existence of two types of asynchronous network states as reported in a recent paper. We also found splitting of the coefficient of variation distribution at the transition point that showed that beyond the transition point the neural population splits in two. The input-output characteristics of the network were studied in response to various types of input pulses. We observed that before the transition point the network efficiently transmits the signal and beyond the transition point it transforms the input which was also reported in a study.



## Chapter 1

# Introduction

### 1.1 History of Neural Networks

By the middle of the 19<sup>th</sup> century, it was known that plant and animal tissues consisted of discrete functional units called “cells”. When the nerve tissue was observed under a microscope, cell bodies having many tangled projections were found. It was concluded from these observations that the fibers emerging from different cell bodies fused to form a continuous network known as “Reticulum” (Figure 1.1 (a)). Reticular theory [1] of the brain was accepted at that time and brain couldn’t be split into distinct structural units.

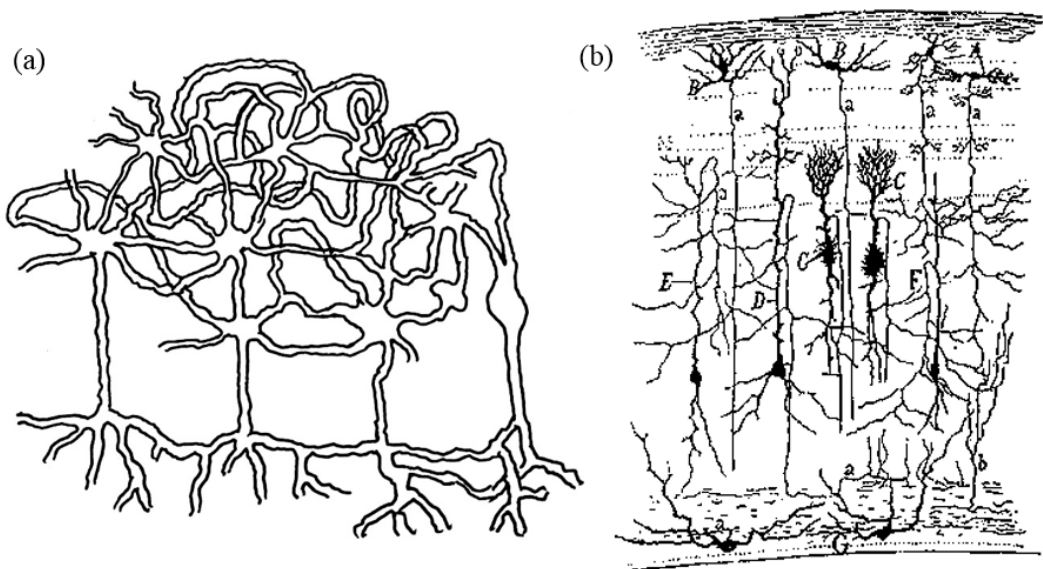


Figure 1.1 (a) Depiction of reticular brain structure, (b) Sketch of real neural network by Ramón y Cajal [2]

In 1887, Santiago Ramón y Cajal used an inefficient stain, which was discovered by Camillo Golgi, that stained only a few cell bodies and their processes in the tissue sample. This method revealed the complete single cell structure and its exact arrangement within the tissue in the background of unstained tissue. Cajal made detailed sketches of single cells which were called “Neurons”. He also made sketches of neural networks within the tissue (Figure 1.1 (b)) and this was the first evidence of the existence of network structure within the nervous system and this discovery marked an end to the Reticular theory.

## 1.2 Biological Neuron

A neuron is an example of electrically excitable system. It is the fundamental unit of computation in the nervous system. The currency of information exchange among neurons is action potential or a spike. The electrical excitability arises from the interplay of various time constants governing kinetics of various channels embedded within neuronal membranes. Every neuron has three basic structures (Figure 1.2(a)):

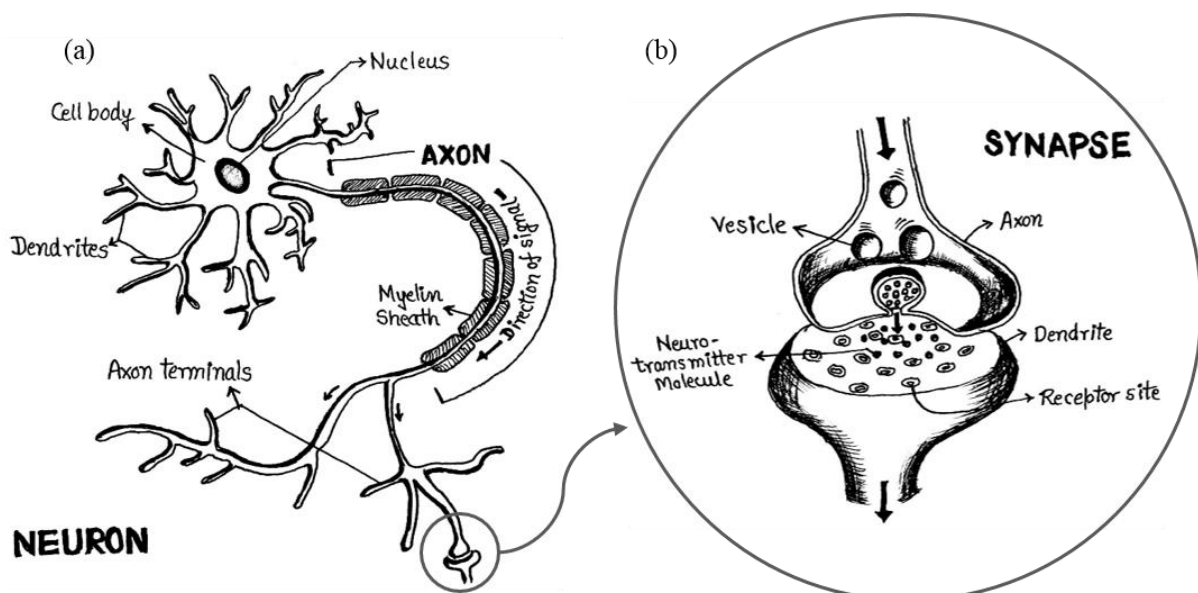


Figure 1.2 (a) Structure of single neuron, (b) Structure of synapse

- **Dendrites:** Dendrites are tree-like structures found in neurons. The dendritic branches receive inputs from other neurons via synapses.
- **Cell body (Soma):** Cell body is a globular structure found in neurons where all inputs from dendritic branches are integrated and processed.
- **Axon:** This is the output end of the neuron which transmits spikes to other neurons via synapses.

Once the membrane potential reaches a certain value, also known as the firing threshold of the neuron, an action potential is emitted. Neurons communicate with one another via synapses (Figure 1.2 (b)) which can be either excitatory (depolarizing the postsynaptic membrane) or inhibitory (hyperpolarizing the postsynaptic membrane) depending on the type of neurotransmitters released by the presynaptic neuron.

### 1.3 Modeling Neurons as RC circuits

Biological cell membranes are phospholipid bilayers with channels and pumps embedded within them. Neuronal membranes are no exceptions. Lipid bilayers are organized in such a manner that the hydrophobic parts of lipids form the interior and hydrophilic heads form the exterior of the membrane (Figure 1.3). The membrane separates intracellular space from extracellular space and helps to maintain the ionic gradients with the help of ion pumps. This configuration is same as that of a capacitor where the two charged sides (intracellular and extracellular space) are separated by a dielectric medium (the hydrophobic interior of lipid bilayer).

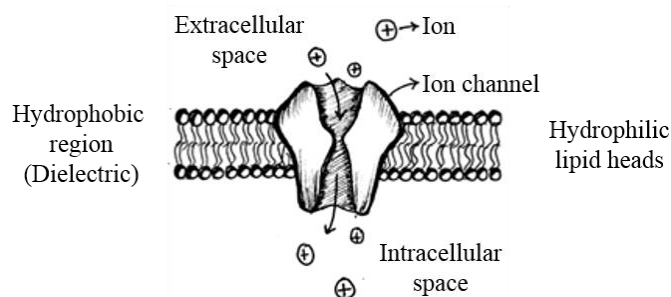


Figure 1.3 Structure of a patch of cell membrane

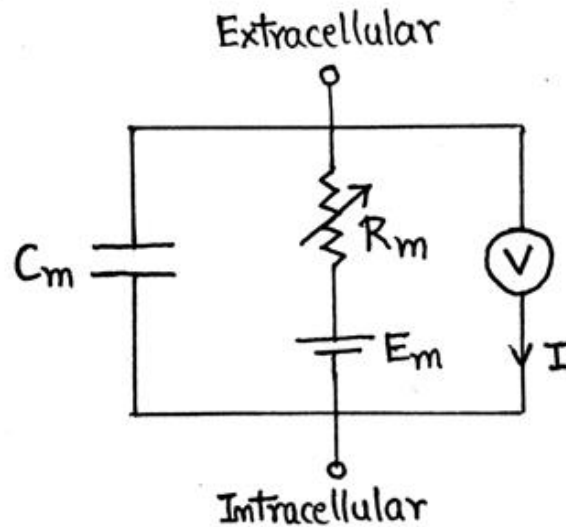


Figure 1.4 Equivalent RC circuit of cell membrane

Various factors (membrane potential, mechanical force, ligand binding etc.) affect the opening and closing of the channels embedded within the membrane and offer variable resistance to ionic currents flowing through them depending on their opening and closing kinetics. Thus, a patch of the membrane can be thought of as parallel RC circuits connected in series (Figure 1.3 (b)).

## 1.4 Leaky Integrate-and-Fire Model

When current is applied to a patch of membrane, it charges like an equivalent RC circuit. Hence neuronal membrane can be thought of as an RC circuit with added spike generation and reset mechanism [3]. Subthreshold voltage evolution is given by:

$$C_m \frac{dV}{dt} = -\frac{V - E_m}{R_m} + I$$

where,  $C_m$  is the membrane capacitance,  $R_m$  is the membrane resistance and  $I$  is the total current flowing across the cell membrane. Above equation can be rewritten in terms of membrane time constant  $\tau_m$ , which is the product of  $C_m$  and  $R_m$ , as:

$$\tau_m \frac{dV}{dt} = -V + E_m + R_m I \tag{1.1}$$

Once spike generation and reset mechanisms are added to passive membrane dynamics, we get the “Integrate and Fire” model of neuron which is shown below (Figure 1.4)

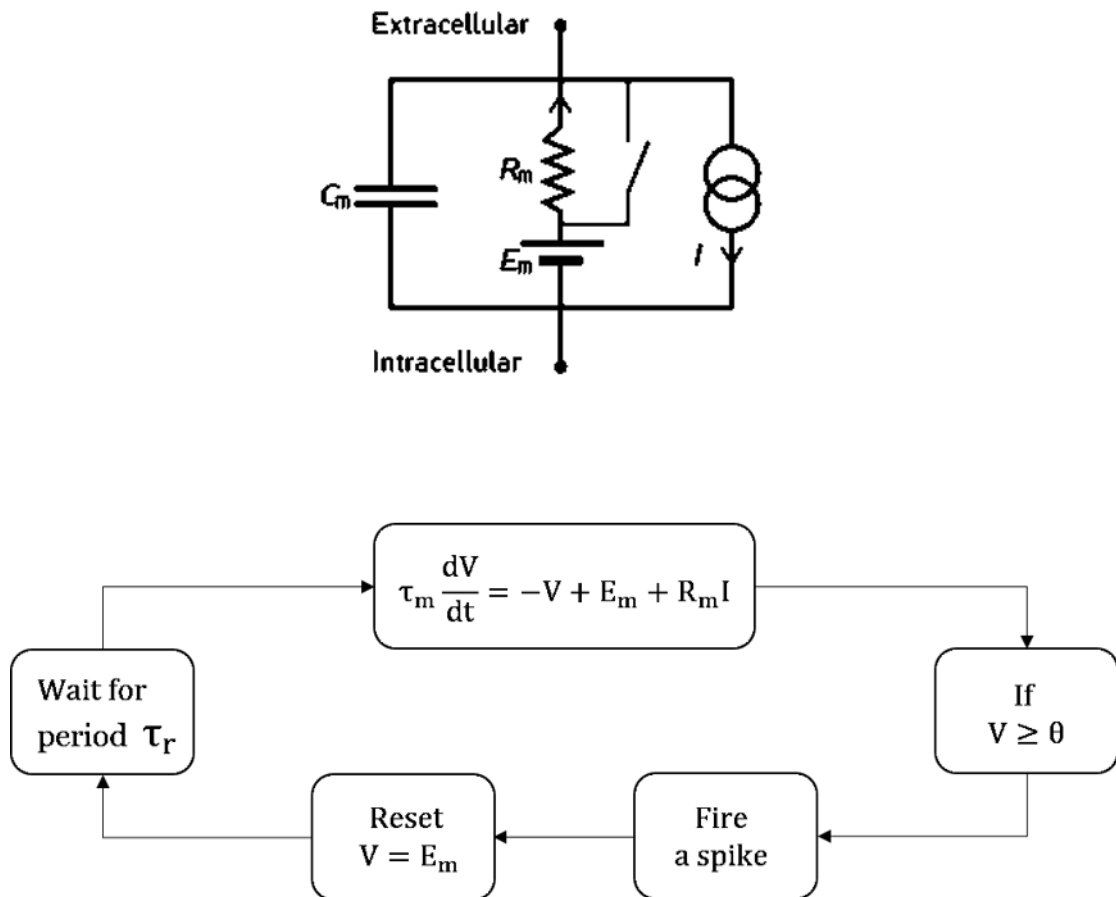


Figure 1.5 Integrate-and-fire model of single neuron and its equivalent circuit diagram [7]

When the membrane potential  $V$  reaches the firing threshold, the neuron fires a spike and the membrane potential  $V$  is reset to  $E_m$  followed by an absolute refractory period ( $\tau_r$ ) during which neuron is inactive.

## 1.5 Response of Integrate-and-Fire Neuron to Square Pulse

### 1.5.1 Membrane response at various membrane time constants

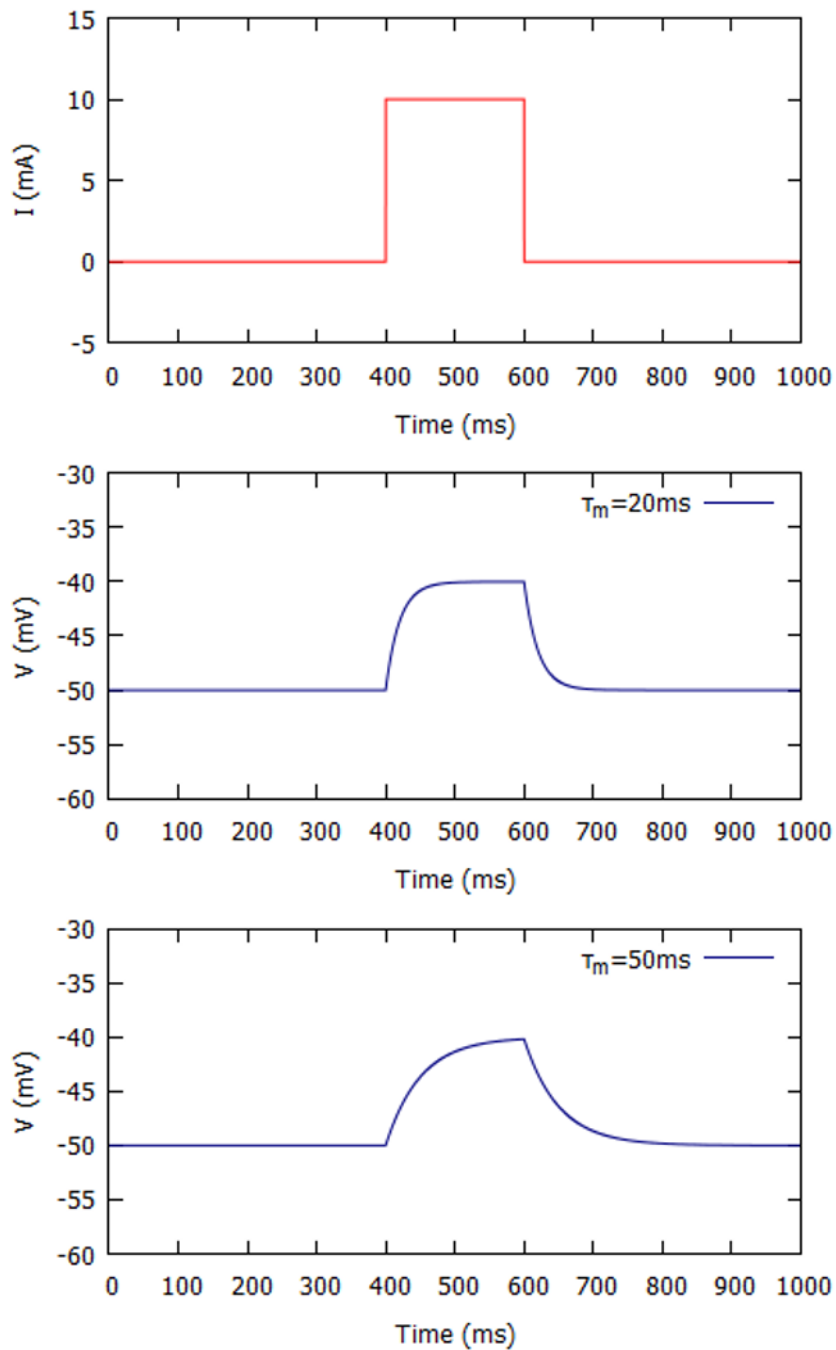


Figure 1.6 Response of membrane patch to input square pulse at two different membrane time constants ( $\tau_m$ ): 20ms and 50ms



## 1.5.2 Membrane response at various current amplitudes

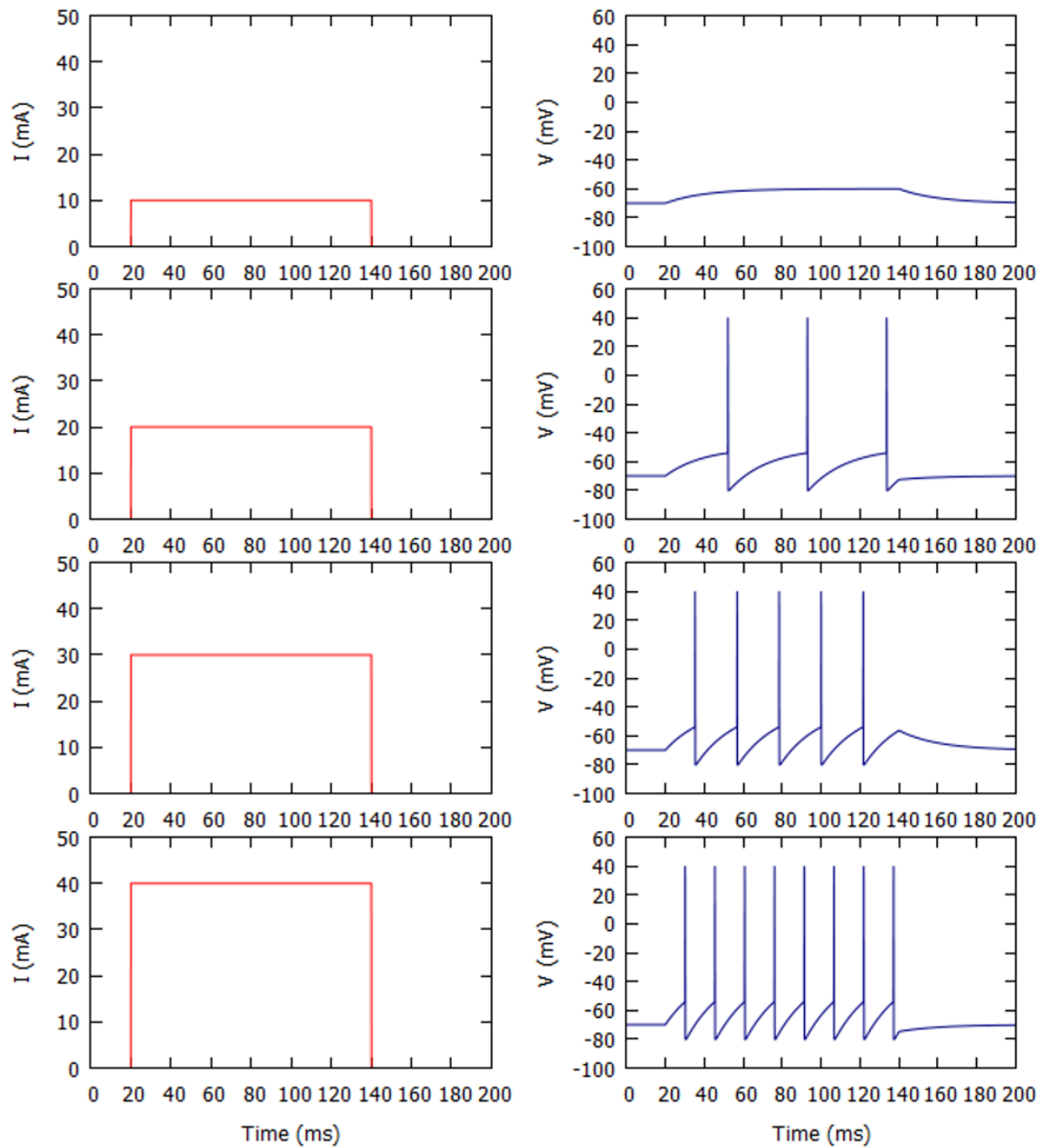


Figure 1.7 Response of single integrate-and-fire neuron to input current pulses of four different amplitudes: 10mA, 20mA, 30mA and 40mA. Here,  $T=200\text{ms}$ ,  $\tau_m=20\text{ms}$ ,  $\tau_r=0.5\text{ms}$ ,  $E_m = -70\text{mV}$ ,  $V_{\text{reset}} = -80\text{mV}$  and  $\theta = -54 \text{ mV}$ ,  $R_m = 1\Omega$

## 1.6 Frequency – Current Curve of Integrate-and Fire Neuron

The general solution of integrate-and-fire model can be given as:

$$V(t) = V_0 e^{-\frac{t-t_0}{\tau_m}} + e^{-\frac{t}{\tau_m}} \int_{t_0}^t e^{\frac{t}{\tau_m}} \left[ \frac{E_m + R_m I(t)}{\tau_m} \right] dt$$

If the external driving current is constant then the exact solution of integrate and fire model is:

$$V(t) = E_m + R_m I + [V_0 - E_m - R_m I] e^{-\frac{t-t_0}{\tau_m}} \quad (1.2)$$

Spikes do not appear yet in the model. Spikes can be added by an additional threshold mechanism. Let  $t_0 = 0$ ,  $V_0 = E_m$  and  $\theta$  be the threshold of the neuron, time to first spike can be calculated as:

$$\theta = E_m + R_m I \left[ 1 - e^{-\frac{T_s}{\tau_m}} \right]$$

$$T_s = -\tau_m \ln \left[ 1 - \frac{\theta - E_m}{R_m I} \right]$$

The interval between consecutive spikes during constant current injection is the sum of time to first spike and the absolute refractory period,  $T_s + \tau_r$ . The firing frequency  $f(I)$  is the reciprocal of this interval:

$$f(I) = \frac{1}{T_s + \tau_r} = \frac{1}{\tau_r - \tau_m \ln \left[ 1 - \frac{\theta - E_m}{R_m I} \right]} \quad (1.3)$$

This is called f-I curve of integrate-and-fire neuron [7] (Figure 1.8)

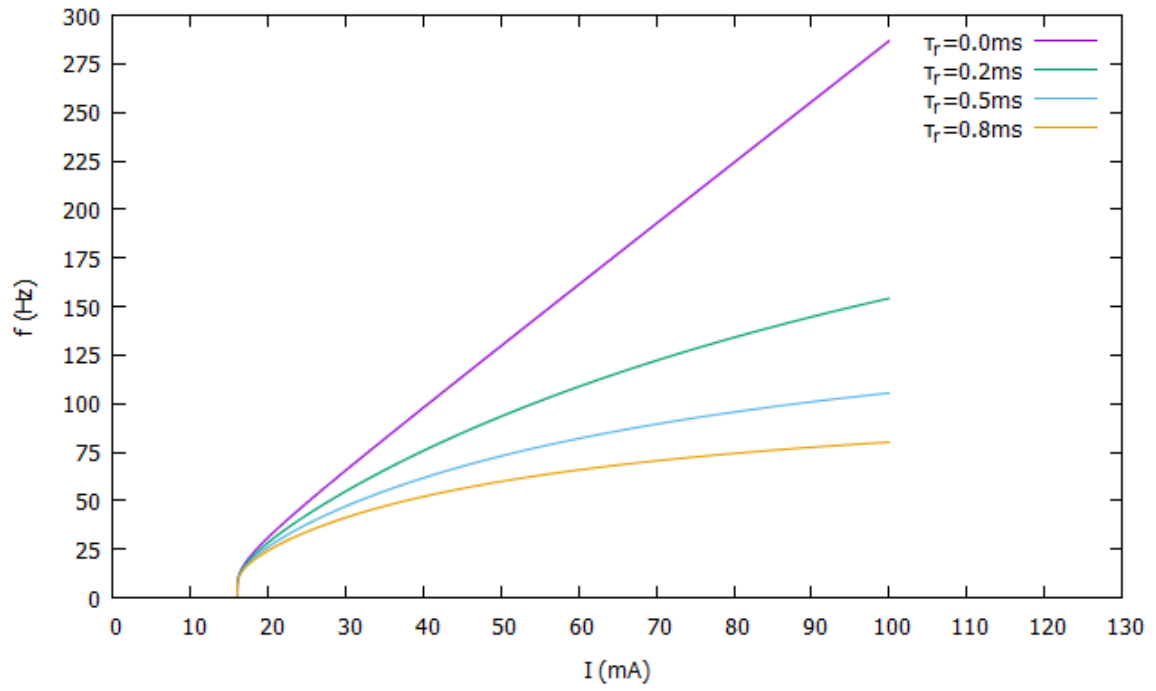


Figure 1.8 Frequency – Current (f-I) curve for integrate-and –fire neuron at four different refractory periods ( $\tau_r$ ): 0ms,0.2ms,0.5ms and 0.8ms



## Chapter 2

# Network of Neurons

## 2.1 Networks and their representation

In general, a network, also called “Graph” is a collection of vertices joined by edges. We are interested in directed and weighted graph where the vertices are neurons and edges are the synapses with assigned synaptic weight [8].

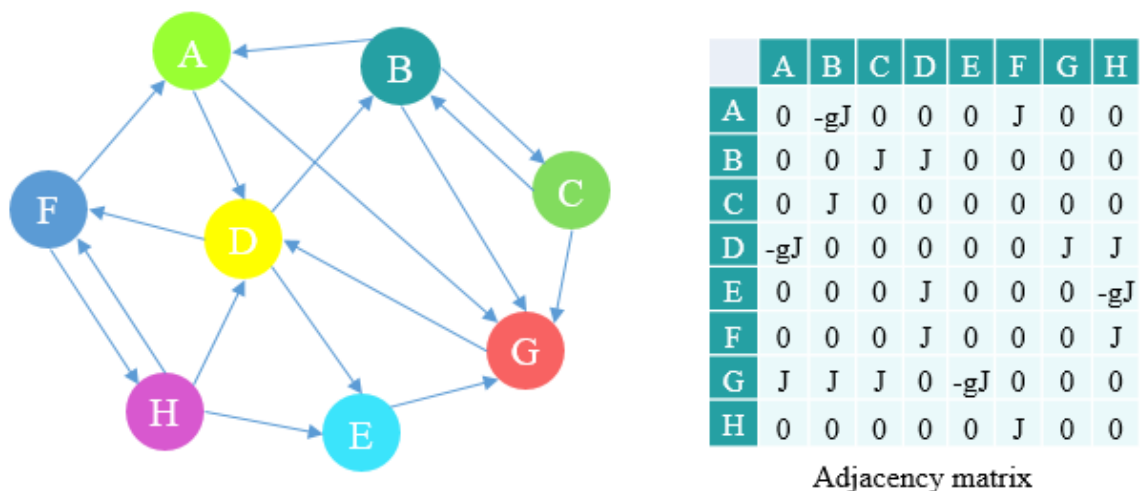


Figure 2.1 Directed network with 8 nodes and 17 edges and corresponding adjacency matrix

## 2.2 The Adjacency Matrix

Let  $n$  be the number of nodes in a network and  $(i, j)$  be the edge between two nodes  $i$  and  $j$ , then the network can be fully specified by  $n$  and a list of all edges  $(i, j)$ . Such a

specification is called an edge list. Mathematics of networks in terms of edge list is cumbersome. A better way of representing networks is adjacency matrix. The adjacency matrix  $A$  of a graph is a  $n \times n$  matrix with elements  $A_{ij}$  such that

$$A_{ij} = \begin{cases} J_{ij}, & \text{if connection exist from } j^{\text{th}} \text{ node to } i^{\text{th}} \text{ node} \\ 0, & \text{otherwise} \end{cases}$$

where,  $J_{ij}$  is the weight of connection from  $j^{\text{th}}$  node to  $i^{\text{th}}$  node.

Two important points about adjacency matrix are:

1. For a network with no self-edges, the diagonal elements are zero.
2. For the undirected network, the adjacency matrix is symmetric.

## 2.3 Population Activity

In a population of  $N$  neurons, the population activity (Figure 2.2) is calculated by counting the number of spikes  $n_{\text{act}}(t; t + \Delta t)$  in a small interval  $\Delta t$  and dividing by  $N$  [10].

$$A(t) = \lim_{\Delta t \rightarrow 0} \frac{1}{\Delta t} \frac{n_{\text{act}}(t; t + \Delta t)}{N} = \frac{1}{N} \sum_{j=1}^N \sum_f \delta(t - t_j^{(f)}) \quad (2.1)$$

Where  $\delta$  denotes the Dirac-delta function. The double sum runs over all firing times  $t_j^{(f)}$  of all neurons in the population. In other words, the activity  $A$  is defined by a population average.

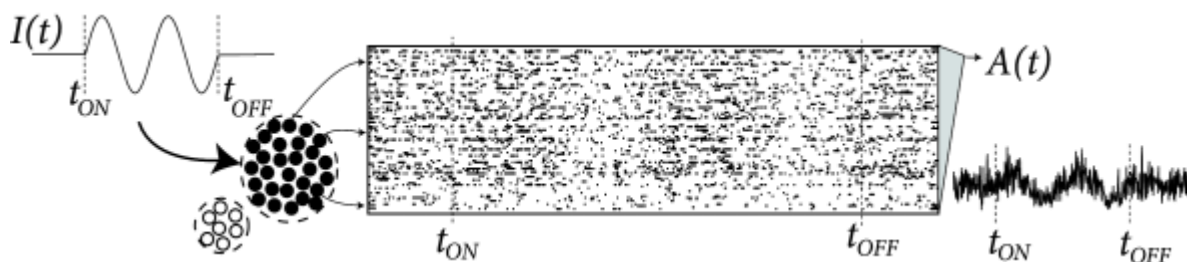


Figure 2.2 Activity of Neuronal population in response to input signal [10]

## 2.4 Homogeneous Population of Integrate-and-Fire Neurons

The dynamics of single integrate-and-fire neuron in the network can be given as:

$$\tau_m \frac{dV_i}{dt} = -V_i + \mu_0 + RI_i(t) + \mu_{\text{ext}}(t) \quad \forall V_i < \theta$$

Integration restarts at  $V_{\text{reset}}$  after the the refractory period  $\tau_r \quad \forall V_i > \theta$

(2.2)

A homogeneous neural network consists of neurons having similar biophysical properties such as input resistance  $R$ , membrane time constant  $\tau_m$ , synaptic time constant  $\tau_s$ , absolute refractory period  $\tau_r$ , firing threshold  $\theta$  and reset potential  $V_{\text{reset}}$ . The total input current to a neuron in the network is the weighted sum of synaptic currents from all other neurons and external current:

$$I_i(t) = \sum_{j=1}^N \sum_f J_{ij} \alpha(t - t_j^{(f)}) + I_{\text{ext}}(t)$$

(2.3)

Here we have assumed that each input spike generates a postsynaptic current with some generic time course  $\alpha(t - t_j^{(f)})$  which is given as:

$$\alpha(t - t_j^{(f)}) = \frac{t}{\tau_s} e^{(1 - \frac{t}{\tau_s})}$$

(2.4)

The sum on the right-hand side of the equation 2.3 runs over all firing times of all neurons. The total input current to all the neurons is identical because of homogeneity of the network. By inserting  $J_{ij} = J$  and using the definition of population activity, the total input current to a neuron can be given as:

$$I(t) = JN \int_0^{\infty} \alpha(s) A(t - s) ds + I_{\text{ext}}(t)$$

(2.5)

This total current is independent of the neuronal index  $i$  as expected due to the homogeneity of the network. Thus, the input current at time  $t$  depends on the past population activity and is the same for all neurons.



## Chapter 3

# Simulations and Results

### 3.1 Network Description and Parameters

The network being studied here is a homogeneous network similar to that studied by Brunel [5]. It consists of  $N$  leaky integrate-and-fire neurons out of which  $N_E$  are excitatory neurons and  $N_I$  are inhibitory neurons. The fraction of excitatory neurons in the network is denoted by  $f$ . Each neuron has an average in-degree  $C(= pN$ , where  $p$  is the sparsity of connections in the network) . Each neuron receives  $C_E(= pN_E)$  excitatory inputs and  $C_I(= pN_I)$  inhibitory inputs. The amplitude of excitatory postsynaptic potential (EPSP) denoted as  $J$  and that of inhibitory postsynaptic potential (IPSP) denoted as  $-gJ$ , where  $g$  is the relative strength of inhibition, is kept same for all the neurons for simplicity. Neurons are connected to each other by alpha synapses. The parameter space of the network consists of the following:

- EPSP amplitude ( $J$ )
- Relative strength of inhibition ( $g$ )
- In-degree of neuron  $I$
- Network size ( $N$ )
- Membrane time constant ( $\tau_m$ )
- Absolute refractory period ( $\tau_r$ )
- Synaptic time constant ( $\tau_s$ )
- Offset current ( $\mu_0$ )

Self-sustained activity in a network of excitatory and inhibitory neurons is one of the intriguing features in neuronal networks. The network displays permanent self-sustained activity only when a current above firing threshold is provided continuously to all neurons and in the absence of such current, the activity decays with time. We studied the self-sustained activity in the network with constant offset current (above firing threshold) being provided to all neurons. The excitatory synapses increase the activity of the network while the inhibitory synapses decrease it. The ratio of number of excitatory to inhibitory neurons is taken as 4:1 which is biologically consistent. Self-sustained asynchronous activity is obtained in the network when inhibition dominates excitation. Thus the strength of IPSP must more than four times than that of EPSP to get such activity. We examined the network properties in the inhibition dominated regime. The network displays a balanced self-sustained asynchronous state and undergoes a transition to another state as the strength of EPSP was increased. This is a heterogeneous asynchronous state where the firing rates of individual neurons show large variation in contrast to the state at low strength of EPSP.

### **3.2 Response of Network as a Function of Network Parameters**

The program for network simulation was written in Julia programming language [9]. Following are the results of simulations where the mean population activity is plotted against the strength of excitation (amplitude of EPSP) at various values of other network parameters indicated within the figures.

### 3.2.1 Average population activity Vs excitation strength ( J ) at various g values

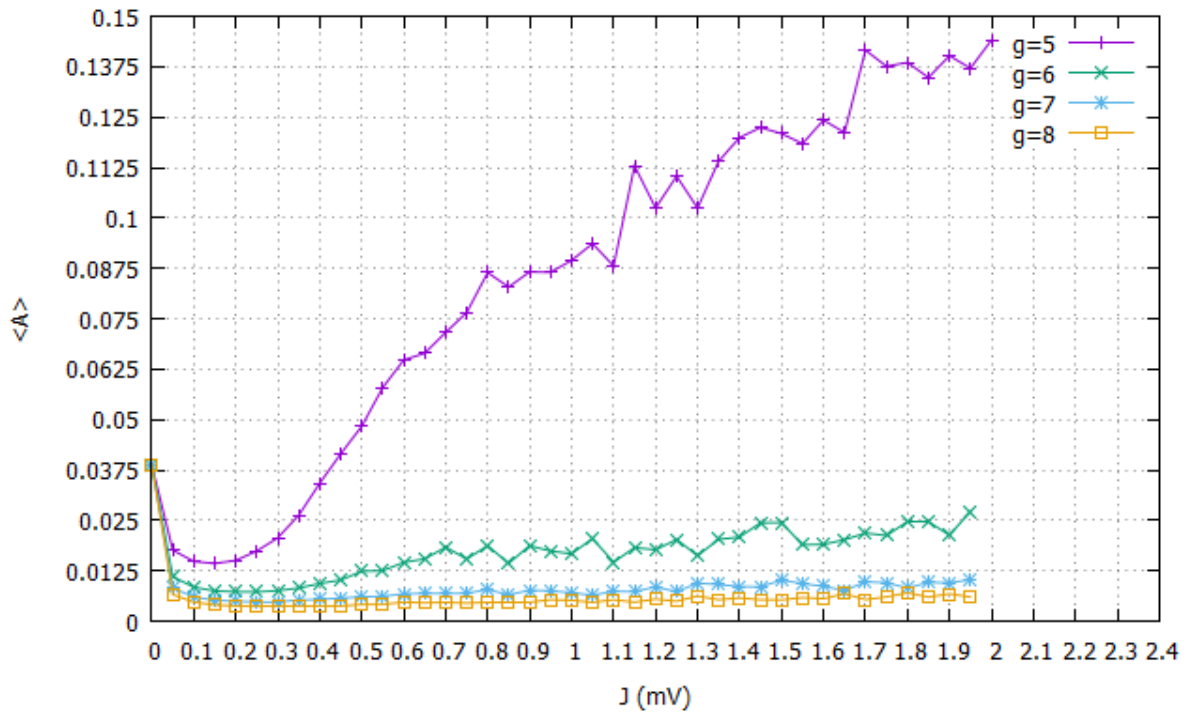


Figure 3.1 Average population activity as a function of strength of EPSP (J) at different relative inhibition strengths(g): 5, 6, 7 and 8. Here,  $f=0.8$ ,  $T=1$  second,  $\mu_0 = 24$  mV,  $V_{\text{reset}}=10\text{mV}$ ,  $\theta = 20$  mV,  $N=10000$ ,  $C=1000$ ,  $\tau_s=0.55\text{ms}$ ,  $\tau_m=20\text{ms}$ ,  $\tau_r=0.5\text{ms}$

The total synaptic input in the network can be represented in vector form as

$$\mathbf{I} = (JA_E - gJA_I)\mathbf{v} \quad (3.1)$$

Where,  $\mathbf{I}$  is  $1 \times N$  synaptic input vector (representing total synaptic input to every neuron in the network),  $\mathbf{v}$  is  $1 \times N$  state vector (representing states of all the neurons in the network),  $A_E$  and  $A_I$  are adjacency matrices of excitatory and inhibitory connections respectively. From equation 3.1, it is clear that increasing the relative strength of inhibition to excitation (g) will decrease total synaptic input to neurons for given J value and hence the overall activity of the network should decrease as g is increased keeping J fixed. It should be noted from the equation above that the difference between activities at two g values will increase with J.

### 3.2.2 Average population activity Vs excitation strength ( J ) at various C values

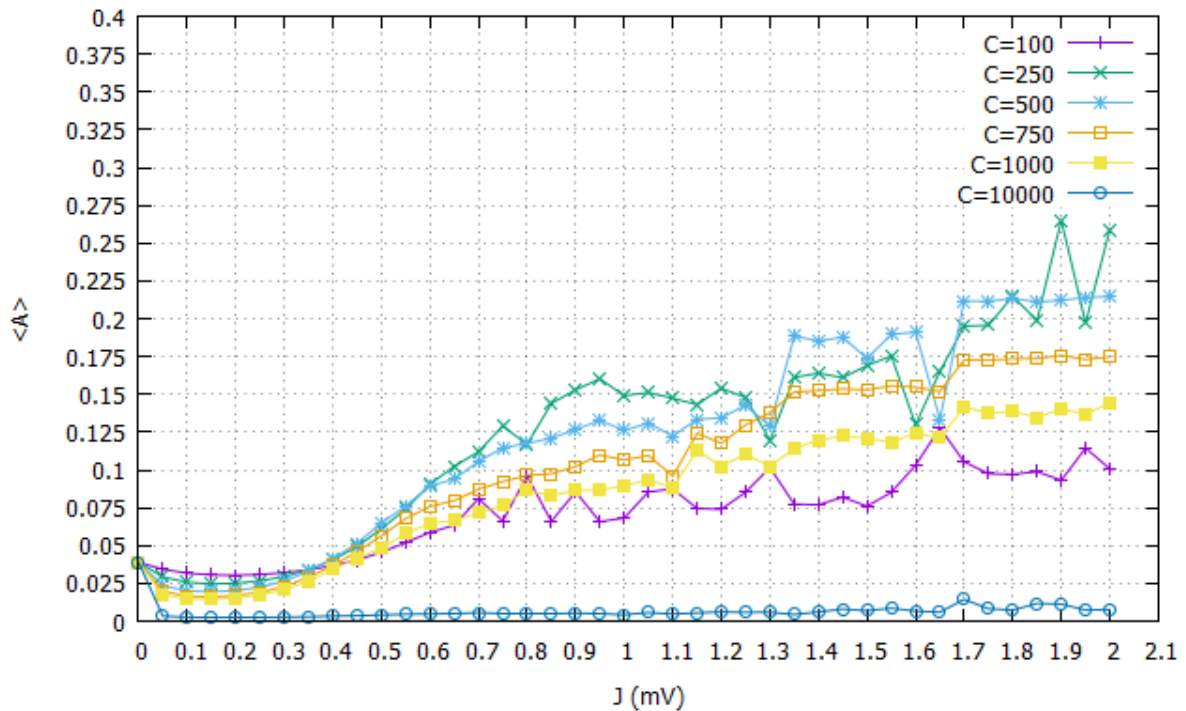


Figure 3.2 Average population activity as a function of the strength of EPSP (J) at different average in-degree per neuron(C): 100, 250, 500, 750, 1000 and 10000. Here,  $f=0.8$ ,  $T=1$  second,  $\mu_0=24\text{mV}$ ,  $V_{\text{reset}}=10\text{mV}$ ,  $\theta =20\text{mV}$ ,  $N=10000$ ,  $g=5$ ,  $\tau_s=0.55\text{ms}$ ,  $\tau_m=20\text{ms}$ ,  $\tau_r=0.5\text{ms}$

General conclusions about the effects of changing the in-degree of neurons cannot be made as the phase curves does not follow a trend consistent with all values of C. Simulations show that all the graphs intersect each other at the same point around  $J=0.4\text{mV}$ . This point is reported as critical excitation strength beyond which transition from classical asynchronous state to heterogeneous asynchronous state takes place. The network activity starts with a limiting value of around 0.037 at zero coupling due to constant offset current being provided to all neurons. As the excitation strength (J) increases the firing frequency goes down initially. This decrease at weak excitation strengths is predicted by mean field theory. Beyond a certain strength of excitation, the network activity diverges from the mean field prediction and again starts to increase [4].

### 3.2.3 Average population activity Vs excitation strength ( J ) at various N values

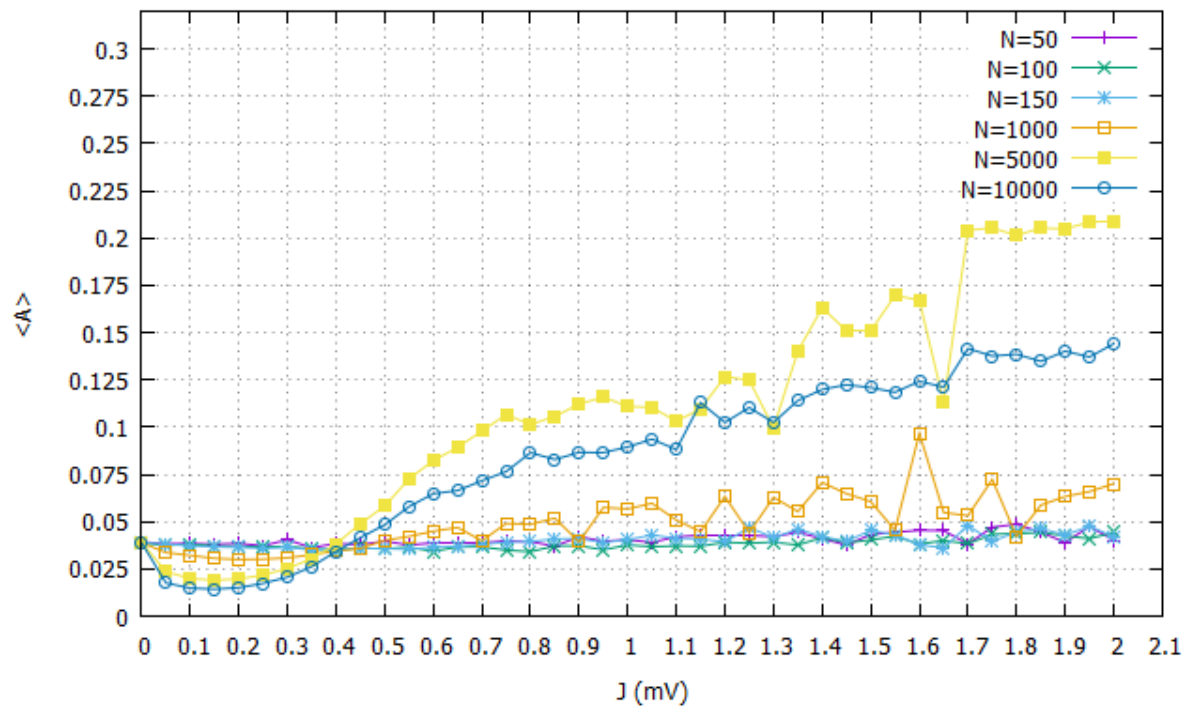


Figure 3.3 Average population activity as a function of the strength of EPSP (J) at different network sizes (N): 50, 100, 150, 1000, 5000 and 10000. Here,  $f=0.8$ ,  $T=1$  second,  $\mu_0 = 24$  mV,  $V_{\text{reset}}=10$ mV,  $\theta = 20$  mV,  $g=5$ ,  $C=1000$ ,  $\tau_s=0.55$ ms,  $\tau_m=20$ ms,  $\tau_r=0.5$ ms

The effects of network size are not very clear. General conclusions cannot be made about the effect of network size on the phase curves. The trends followed by these curves are not consistent with all the values of network sizes. Although we cannot conclude much, we definitely observe finite size effects in the results for small network sizes. For small networks, the activity looks almost flat across J but as the size increases we start seeing the variations across J. Again we observe the intersecting of all the phase curves at the same critical point about  $J=0.4$ mV [4].

### 3.2.4 Average population activity Vs excitation strength ( J ) at various $\tau_m$ values

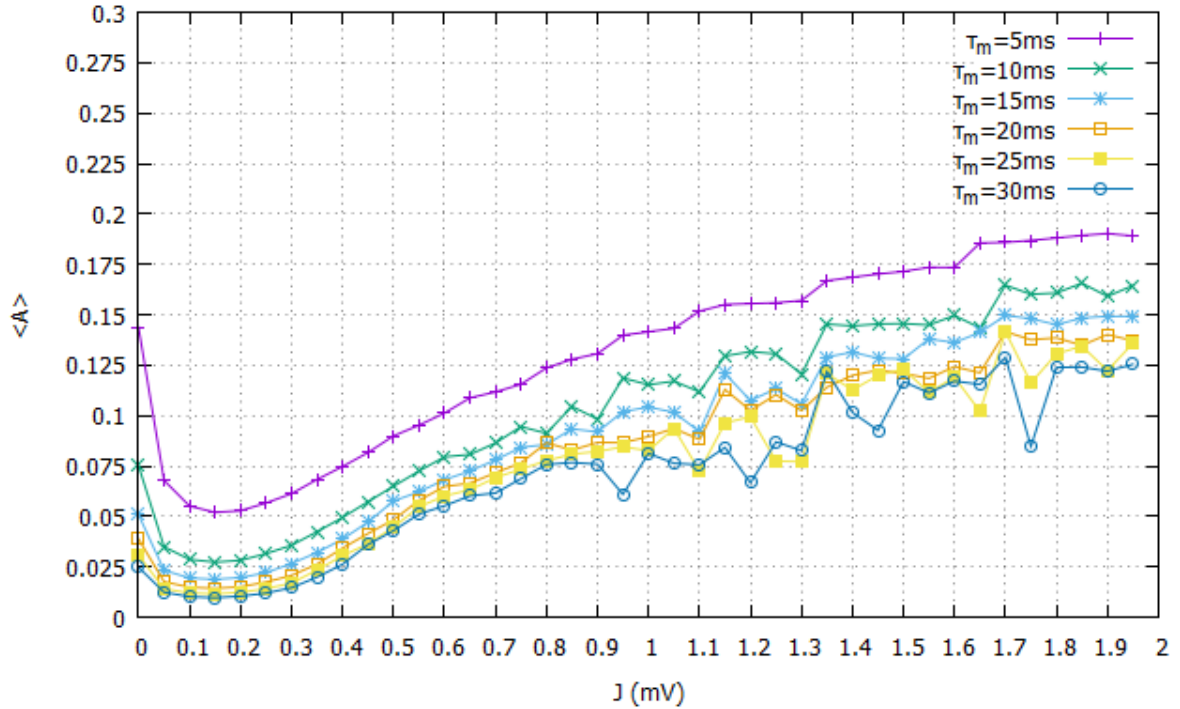


Figure 3.4 Average population activity as a function of strength of EPSP (J) at different membrane time constants ( $\tau_m$ ): 5ms, 10ms, 15ms, 20ms, 25ms and 30ms. Here,  $f=0.8$ ,  $T=1$  second,  $\mu_0=24mV$ ,  $V_{reset}=10mV$ ,  $\theta=20mV$ ,  $N=10000$ ,  $C=1000$ ,  $g=5$ ,  $\tau_s=0.55ms$ ,  $\tau_r=0.5ms$

Membrane time constant in an RC circuit defines the speed of charging and discharging of the capacitor. Similarly, for a neuron, higher time constant will result in the longer time interval between successive spikes or decreased firing frequency (Equation 1.3). Hence, increasing membrane time constant while keeping all the other parameters fixed will result in decreased population activity for all J values. So, the graphs should shift vertically downwards as  $\tau_m$  is increased and the same is observed in the simulations.

### 3.2.5 Average population activity Vs excitation strength ( J ) at various $\tau_r$ values

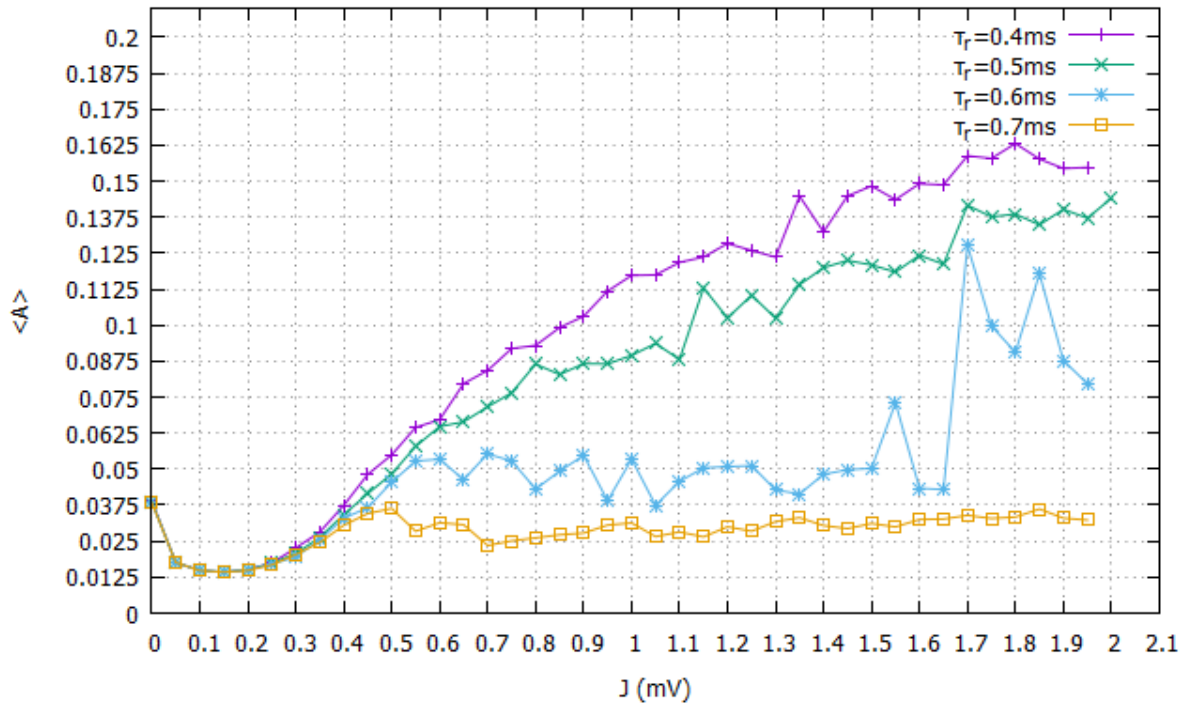


Figure 3.5 Average population activity as a function of strength of EPSP (J) at different refractory periods ( $\tau_r$ ): 0.4ms, 0.5ms, 0.6ms and 0.7ms. Here,  $f=0.8$ ,  $T=1$  second,  $\mu_0 = 24$  mV,  $V_{\text{reset}}=10$ mV,  $\theta = 20$  mV,  $N=10000$ ,  $C=1000$ ,  $g=5$ ,  $\tau_s=0.55$ ms,  $\tau_m=20$ ms

The refractory period is the time during which a neuron is inactive and hence increasing this time will lead to decreased firing frequency of the neuron (Equation 1.3). Therefore, network activity should also decrease which is observed in simulations as well. It should be noted that the difference in the activity of the network for two different refractory periods  $\tau_r$  will increase with J because increasing J will increase synaptic input I (Figure 1.7). Therefore for low values of J, the curves for different values of  $\tau_r$  overlap.

### 3.2.6 Average population activity Vs excitation strength ( J ) at various $\tau_s$ values

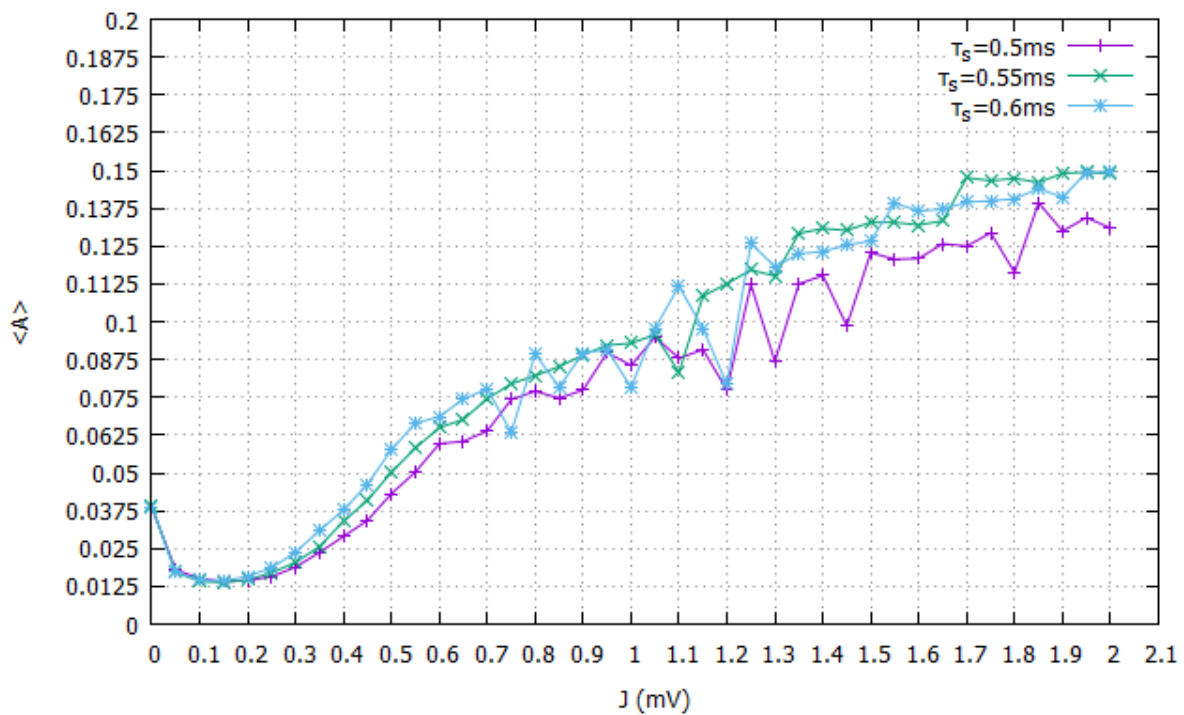


Figure 3.6 Average population activity as a function of strength of EPSP (J) at different synaptic time constants ( $\tau_s$ ): 0.5ms, 0.55ms and 0.6ms. Here,  $f=0.8$ ,  $T=1$  second,  $\mu_0=24$  mV,  $V_{\text{reset}}=10\text{mV}$ ,  $\theta=20$  mV,  $N=10000$ ,  $C=1000$ ,  $g=5$ ,  $\tau_m=20\text{ms}$ ,  $\tau_r=0.5\text{ms}$

Synaptic time constant govern the time course of synaptic conductance which is chosen to be an alpha function (Equation 2.4). Alpha function reaches its maximum value at the time  $\tau_s$ .

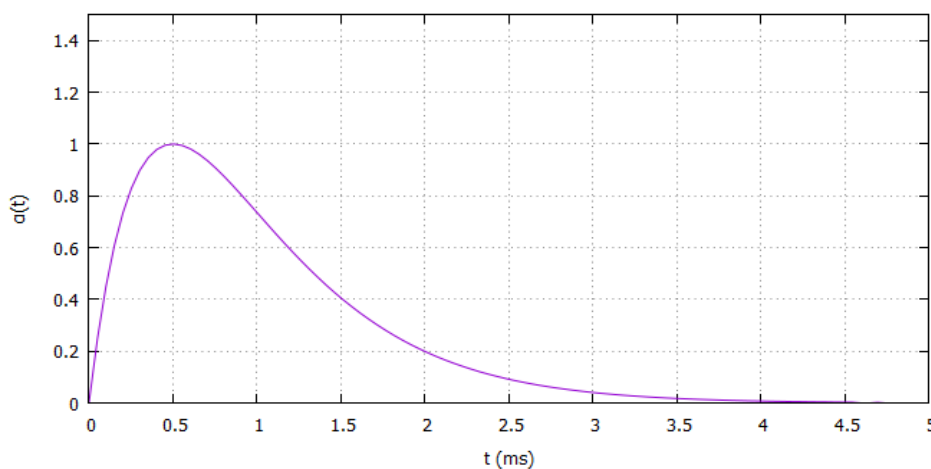


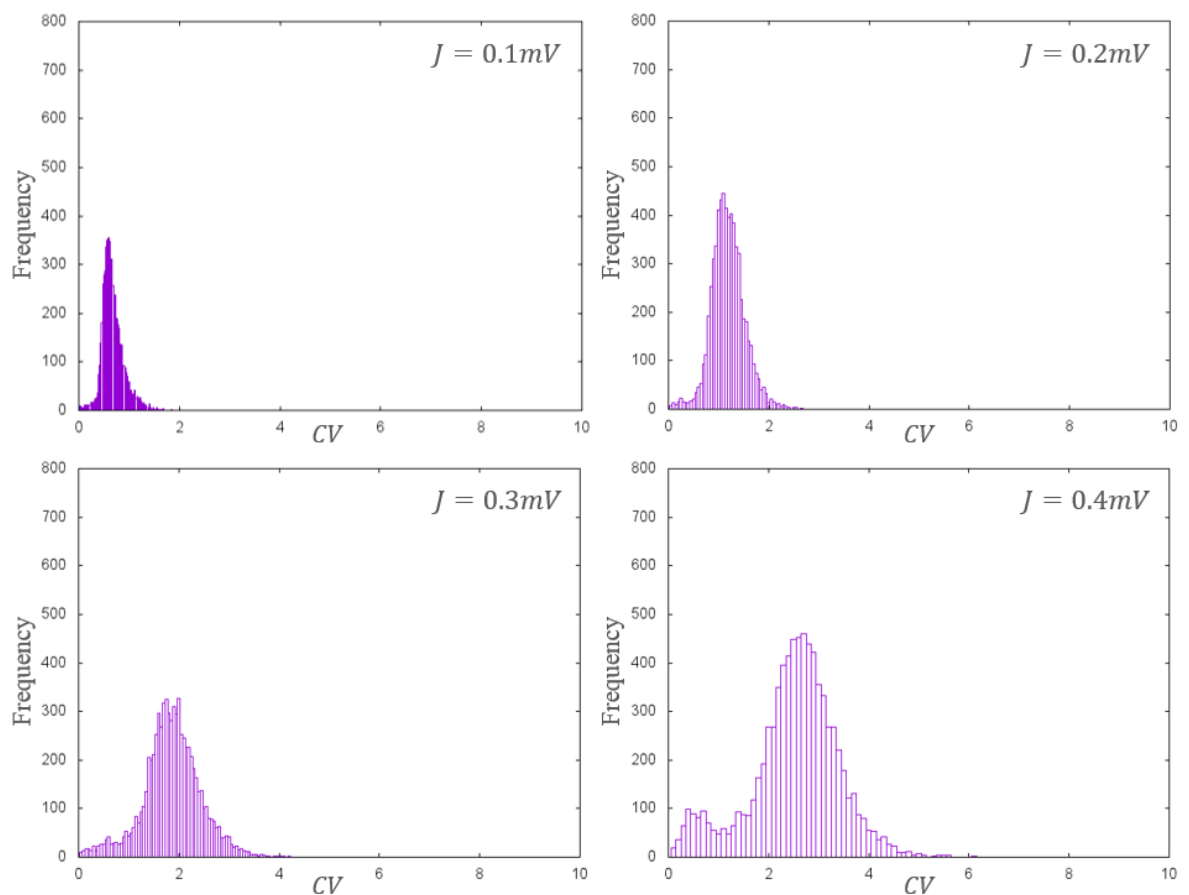
Figure 3.7 Plot of alpha function against time. Here,  $\tau_s=0.5\text{ms}$



Larger the synaptic time constant, longer will it take for alpha function to reach its maximum and the value of the integral on the right-hand side of the Equation 2.5 will increase leading to increase in the total synaptic input. Thus, the effective strength of excitation increases as synaptic time constant is increased leading to increased activity of the network for a given  $J$  value. Therefore, the values of mean population activity will shift leftwards with magnitude proportional to  $J$ , i.e., at lower  $J$  shift will be less and at higher  $J$  shift will be more which is also observed in the simulations.

### 3.3 Splitting of Neural Population

Spike train of each neuron in the network was analyzed to get its interspike interval (ISI) distribution and corresponding coefficient of variation (CV) [6]. Histogram of CVs of all the neurons was plotted as for different strengths of EPSP.



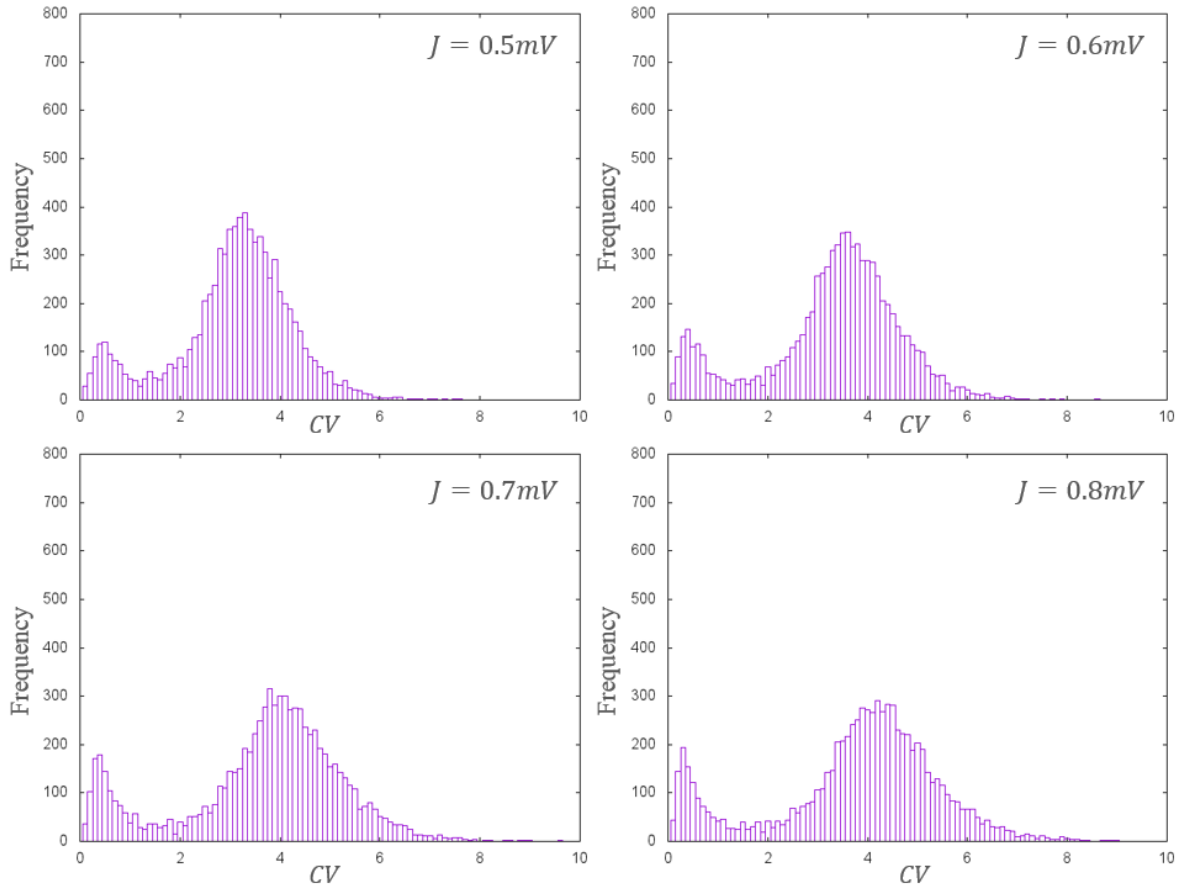


Figure 3.8 Histogram of coefficient of variation of ISI distribution at various strengths of EPSP ( $J$ ) for 10000 neurons. Here,  $f=0.8$ ,  $T=1$  second,  $\mu_0 = 24$  mV,  $V_{\text{reset}}=10\text{mV}$ ,  $\theta = 20$  mV,  $N=10000$ ,  $C=1000$ ,  $g=5$ ,  $\tau_m=20\text{ms}$ ,  $\tau_s=0.55\text{ms}$ ,  $\tau_r=0.5\text{ms}$

These simulations gave interesting results. We saw that as the strength of excitation is increased, the coefficient of variation distribution peak moves to the right (beyond 1) and splits into two (one of them below 1 and other beyond 1) which means that at higher coupling strength the neural population splits into two. This seems to be a good order parameter for the kind of transition taking place in the network. This observation was used as a basis for giving hypothesis related to computational properties of the network.

### 3.4 Network Response to Input Pulses

All the neurons in the network were given short input pulses of various shapes and the population activity was recorded. In all the cases the results showed that at lower couplings the input is reflected in the network output which means the input is getting transmitted through the network in this coupling range and at higher couplings we observe that the network doesn't represent the input signatures in the population activity which mean the network is not efficiently transmitting the input but the input is involved in the complex dynamics going on within the network and is transformed which is useful for doing computations involving inputs.

#### 3.4.1 Gaussian Pulse

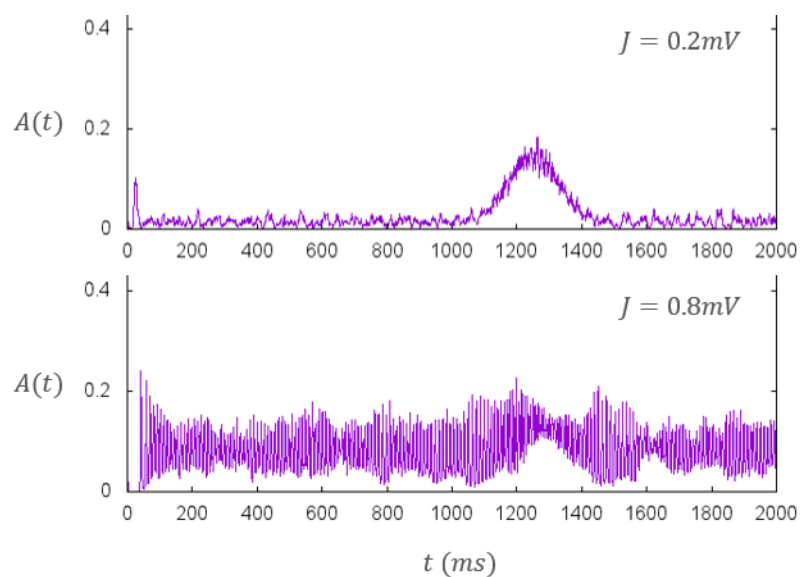


Figure 3.9 Population activity of the network for Gaussian input pulse in two different network states at (a)  $J = 0.2\text{mV}$  (b)  $J = 0.8\text{mV}$ . Here,  $f=0.8$ ,  $T=1$  second,  $\mu_0 = 24$  mV,  $V_{\text{reset}}=10\text{mV}$ ,  $\theta = 20$  mV,  $N=10000$ ,  $C=1000$ ,  $g=5$ ,  $\tau_m=20\text{ms}$ ,  $\tau_s=0.55\text{ms}$ ,  $\tau_r=0.5\text{ms}$

### 3.4.2 Square Pulse

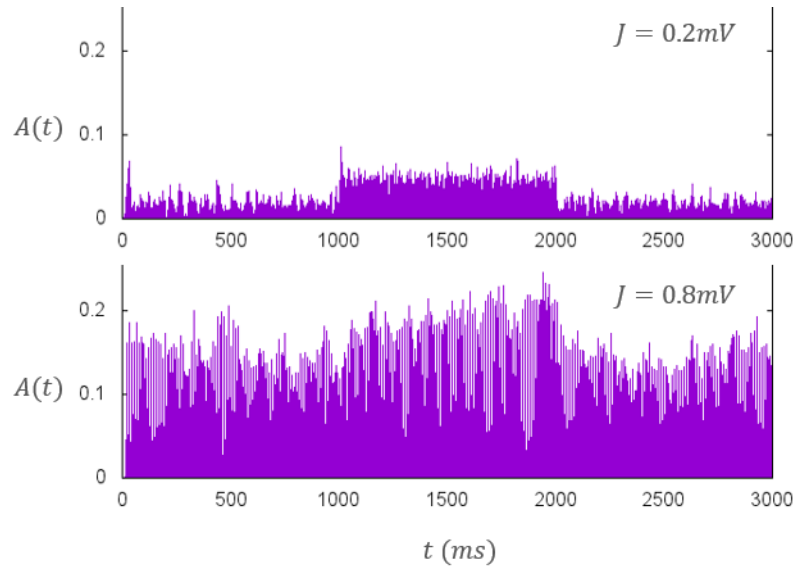


Figure 3.10 Population activity of the network for square input pulse in two different network states at (a)  $J = 0.2\text{mV}$  (b)  $J = 0.8\text{mV}$ . Here,  $f=0.8$ ,  $T=1$  second,  $\mu_0 = 24$  mV,  $V_{\text{reset}}=10\text{mV}$ ,  $\theta = 20$  mV,  $N=10000$ ,  $C=1000$ ,  $g=5$ ,  $\tau_m=20\text{ms}$ ,  $\tau_s=0.55\text{ms}$ ,  $\tau_r=0.5\text{ms}$

### 3.4.3 Ramp Pulse

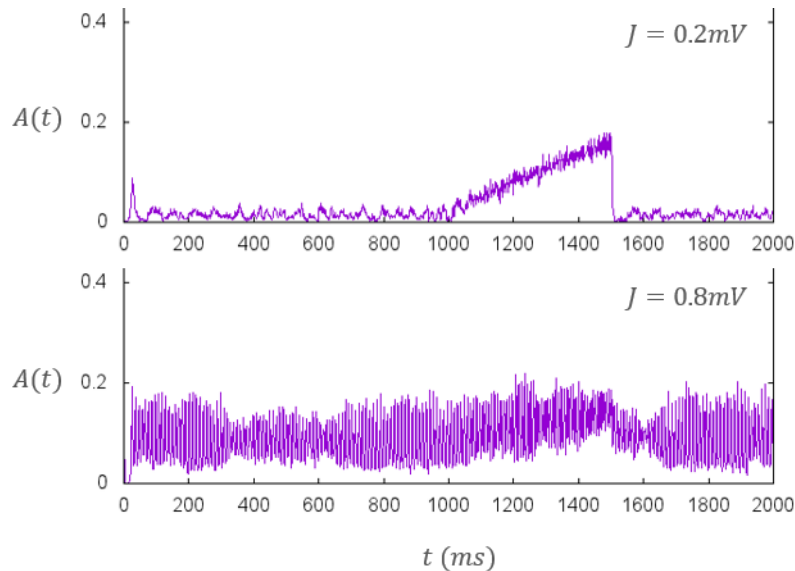


Figure 3.11 Population activity of the network for ramp input pulse in two different network states at (a)  $J = 0.2\text{mV}$  (b)  $J = 0.8\text{mV}$ . Here,  $f=0.8$ ,  $T=1$  second,  $\mu_0 = 24$  mV,  $V_{\text{reset}}=10\text{mV}$ ,  $\theta = 20$  mV,  $N=10000$ ,  $C=1000$ ,  $g=5$ ,  $\tau_m=20\text{ms}$ ,  $\tau_s=0.55\text{ms}$ ,  $\tau_r=0.5\text{ms}$

### 3.4.4 Sinusoidal Pulse

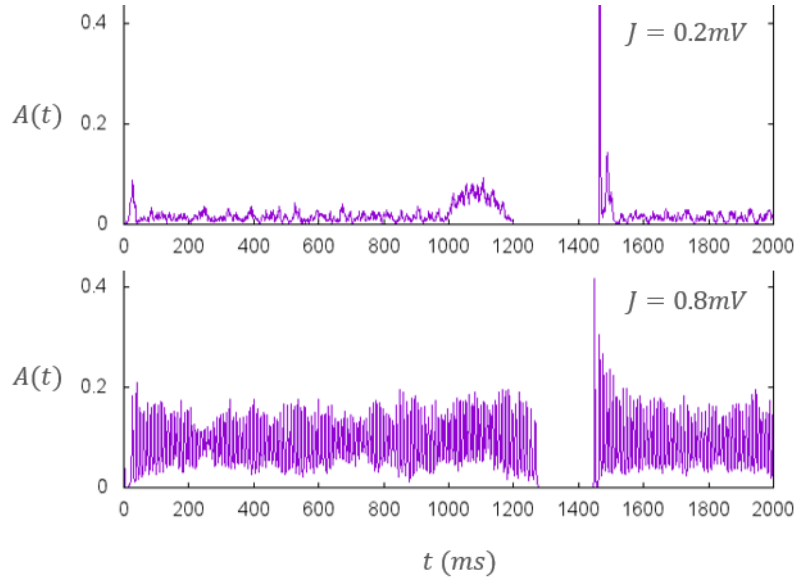


Figure 3.12 Population activity of the network for sinusoidal input pulse in two different network states at (a)  $J = 0.2\text{mV}$  (b)  $J = 0.8\text{mV}$ . Here,  $f=0.8$ ,  $T=1$  second,  $\mu_0 = 24$  mV,  $V_{\text{reset}}=10\text{mV}$ ,  $\theta = 20$  mV,  $N=10000$ ,  $C=1000$ ,  $g=5$ ,  $\tau_m=20\text{ms}$ ,  $\tau_s=0.55\text{ms}$ ,  $\tau_r=0.5\text{ms}$

## 3.5 Conclusions

From the splitting of the coefficient of variation distribution, we concluded that the neural population splits into two beyond a certain strength of EPSP. We also observed that the input is not reflected in the output of the network beyond the same strength of EPSP. Based on these two observations, we hypothesized that till the CV distribution splits, the neural population is transmitting the input as the population and as the splitting occurs, the population splits into two where one population with  $CV \leq 1$  transmits the signal and the other population  $CV > 1$  transforms the input. As a preliminary approach, we considered the total network output to be the linear combination of the outputs from both the populations.

For testing above hypothesis, we took separate outputs from the groups having  $CV < 1$  and  $CV > 1$ . Simulation results were strange. At low coupling  $CV < 1$  group transmits the signal more as compared to  $CV > 1$  (just because there are very few number

of neurons with  $CV > 1$  in that coupling range) but after the splitting of CV distribution, both the groups show no signature of the input. It is possible that the outputs of the two populations are non-linearly interacting to give the total output. So the hypothesis about one group transmitting the signal and other doing computation doesn't seem right. Although our hypothesis was proven wrong, the observations are noteworthy and we are in the process of designing alternate hypothesis and possible experiments to test them.

To summarize, in this project we studied the properties of a balanced network of excitatory and inhibitory neurons as a function of the network parameters and attempted to explain the observations. The network displays two kinds of asynchronous states which have different computational properties. The coefficient of variation distribution seems to be a better order parameter for observing the phase transition than the average population activity. The results obtained in this study are not only limited to neural networks. They can be applied to networks of RC circuits or any other network where the nodes follow the similar form of equations.

---

# References

- [1] [https://en.wikipedia.org/wiki/Reticular\\_theory](https://en.wikipedia.org/wiki/Reticular_theory)
- [2] [https://www.nobelprize.org/nobel\\_prizes/medicine/laureates/1906/cajal-rticle.html](https://www.nobelprize.org/nobel_prizes/medicine/laureates/1906/cajal-rticle.html)
- [3] Abbott, L.F. (1999). "Lapique's introduction of the integrate-and-fire model neuron (1907)" (PDF). *Brain Research Bulletin*. 50 (5/6): 303–304.
- [4] "Two types of asynchronous activity in networks of excitatory and inhibitory spiking neurons", Srdjan Ostojic, *Nature Neuroscience* 17, 594–600 (2014) doi:10.1038/nn.3658
- [5] "Dynamics of Sparsely Connected Networks of Excitatory and Inhibitory Spiking Neurons", Brunel N1, *J Comput Neurosci*. 2000 May-Jun;8(3):183-208.
- [6] *Theoretical Neuroscience Computational and Mathematical Modeling of Neural Systems* - Peter Dayan, L. F. Abbott
- [7] *Principles of Computational modelling in Neuroscience* - David Sterratt, Bruce Graham, Andrew Gillies, David Willshaw
- [8] *Networks: An Introduction* – Mark Newman
- [9] <http://docs.julialang.org/en/release-0.5/manual/>
- [10] *Neuronal Dynamics: From single neurons to networks and models of cognition* - Wulfram Gerstner, Werner M. Kistler, Richard Naud and Liam Paninski